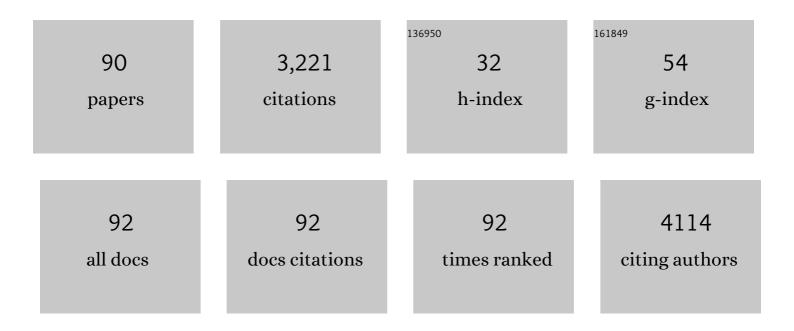


List of Publications by Year in descending order

Source: https://exaly.com/author-pdf/2315799/publications.pdf Version: 2024-02-01



VI ZANIC

#	Article	IF	CITATIONS
1	Small-molecule fluorescence-based probes for interrogating major organ diseases. Chemical Society Reviews, 2021, 50, 9391-9429.	38.1	176
2	The Notch ligand Jagged2 promotes lung adenocarcinoma metastasis through a miR-200–dependent pathway in mice. Journal of Clinical Investigation, 2011, 121, 1373-1385.	8.2	172
3	miR-200 Inhibits Lung Adenocarcinoma Cell Invasion and Metastasis by Targeting <i>Flt1/VEGFR1</i> . Molecular Cancer Research, 2011, 9, 25-35.	3.4	166
4	Remote light-controlled intracellular target recognition by photochromic fluorescent glycoprobes. Nature Communications, 2017, 8, 987.	12.8	141
5	Selective fluorogenic imaging of hepatocellular H ₂ S by a galactosyl azidonaphthalimide probe. Chemical Communications, 2015, 51, 3653-3655.	4.1	121
6	Photochromic Fluorescent Probe Strategy for the Super-resolution Imaging of Biologically Important Biomarkers. Journal of the American Chemical Society, 2020, 142, 18005-18013.	13.7	118
7	Fluorogenic Probing of Specific Recognitions between Sugar Ligands and Glycoprotein Receptors on Cancer Cells by an Economic Graphene Nanocomposite. Advanced Materials, 2013, 25, 4097-4101.	21.0	113
8	Fluorescent probes for the detection of disease-associated biomarkers. Science Bulletin, 2022, 67, 853-878.	9.0	110
9	Carbohydrate CuAAC click chemistry for therapy and diagnosis. Carbohydrate Research, 2016, 429, 1-22.	2.3	109
10	Probing disease-related proteins with fluorogenic composite materials. Chemical Society Reviews, 2015, 44, 4239-4248.	38.1	108
11	Targeted Intracellular Production of Reactive Oxygen Species by a 2D Molybdenum Disulfide Glycosheet. Advanced Materials, 2016, 28, 9356-9363.	21.0	108
12	Fluorogenic Resveratrol-Confined Graphene Oxide For Economic and Rapid Detection Of Alzheimer's Disease. ACS Applied Materials & Interfaces, 2014, 6, 5379-5382.	8.0	79
13	Sensors, Imaging Agents, and Theranostics to Help Understand and Treat Reactive Oxygen Species Related Diseases. Small Methods, 2019, 3, 1900013.	8.6	72
14	Hepatoma-selective imaging of heavy metal ions using a â€~clicked' galactosylrhodamine probe. Chemical Communications, 2014, 50, 11735-11737.	4.1	69
15	Design, synthesis and biological evaluation of colchicine derivatives as novel tubulin and histone deacetylase dual inhibitors. European Journal of Medicinal Chemistry, 2015, 95, 127-135.	5.5	69
16	Fluorescent glycoprobes: a sweet addition for improved sensing. Chemical Communications, 2017, 53, 82-90.	4.1	62
17	The discovery of colchicine-SAHA hybrids as a new class of antitumor agents. Bioorganic and Medicinal Chemistry, 2013, 21, 3240-3244.	3.0	61
18	Glycosylation enhances the aqueous sensitivity and lowers the cytotoxicity of a naphthalimide zinc ion fluorescence probe. Chemical Communications, 2015, 51, 11852-11855.	4.1	59

#	Article	IF	CITATIONS
19	AICAR Induces Astroglial Differentiation of Neural Stem Cells via Activating the JAK/STAT3 Pathway Independently of AMP-activated Protein Kinase. Journal of Biological Chemistry, 2008, 283, 6201-6208.	3.4	56
20	Metal–organic frameworks (MOFs) as host materials for the enhanced delivery of biomacromolecular therapeutics. Chemical Communications, 2021, 57, 12098-12110.	4.1	51
21	Protein encapsulation: a new approach for improving the capability of small-molecule fluorogenic probes. Chemical Science, 2020, 11, 1107-1113.	7.4	49
22	An ultrasensitive fluorogenic probe for revealing the role of glutathione in chemotherapy resistance. Chemical Science, 2017, 8, 8012-8018.	7.4	48
23	AMP-activated Protein Kinase Is Involved in Neural Stem Cell Growth Suppression and Cell Cycle Arrest by 5-Aminoimidazole-4-carboxamide-1-Î ² -d-ribofuranoside and Glucose Deprivation by Down-regulating Phospho-retinoblastoma Protein and Cyclin D. Journal of Biological Chemistry, 2009. 284. 6175-6184.	3.4	45
24	Targeted multimodal theranostics via biorecognition controlled aggregation of metallic nanoparticle composites. Chemical Science, 2016, 7, 4004-4008.	7.4	43
25	One-Step Click Engineering Considerably Ameliorates the Practicality of an Unqualified Rhodamine Probe. ACS Applied Materials & Interfaces, 2014, 6, 19600-19605.	8.0	42
26	Capturing intercellular sugar-mediated ligand-receptor recognitions via a simple yet highly biospecific interfacial system. Scientific Reports, 2013, 3, 2293.	3.3	41
27	Dynamic tracking of pathogenic receptor expression of live cells using pyrenyl glycoanthraquinone-decorated graphene electrodes. Chemical Science, 2015, 6, 1996-2001.	7.4	40
28	A near-infrared fluorescent probe for rapid detection of hydrogen peroxide in living cells. Tetrahedron, 2015, 71, 4842-4845.	1.9	39
29	Cyclodextrin-Based Peptide Self-Assemblies (Spds) That Enhance Peptide-Based Fluorescence Imaging and Antimicrobial Efficacy. Journal of the American Chemical Society, 2020, 142, 1925-1932.	13.7	36
30	Target-Specific Imaging of Transmembrane Receptors Using Quinonyl Glycosides Functionalized Quantum Dots. Analytical Chemistry, 2014, 86, 5502-5507.	6.5	35
31	Substitution Pattern Reverses the Fluorescence Response of Coumarin Glycoligands upon Coordination with Silver (I). Scientific Reports, 2014, 4, 4252.	3.3	34
32	Receptor-targeting fluorescence imaging and theranostics using a graphene oxide based supramolecular glycocomposite. Journal of Materials Chemistry B, 2015, 3, 9182-9185.	5.8	33
33	Foldable glycoprobes capable of fluorogenic crosslinking of biomacromolecules. Chemical Science, 2016, 7, 6325-6329.	7.4	32
34	Phytochemical and biological studies on rare and endangered plants endemic to China. Part XV. Structurally diverse diterpenoids and sesquiterpenoids from the vulnerable conifer. Phytochemistry, 2020, 169, 112184.	2.9	28
35	Regulation of Ubiquitin-like with Plant Homeodomain and RING Finger Domain 1 (UHRF1) Protein Stability by Heat Shock Protein 90 Chaperone Machinery. Journal of Biological Chemistry, 2016, 291, 20125-20135.	3.4	27
36	Quantitative Proteomic Analysis of Membrane Proteins Involved in Astroglial Differentiation of Neural Stem Cells by SILAC Labeling Coupled with LC–MS/MS. Journal of Proteome Research, 2012, 11, 829-838.	3.7	25

#	Article	IF	CITATIONS
37	A general strategy to the intracellular sensing of glycosidases using AIE-based glycoclusters. Chemical Science, 2021, 13, 247-256.	7.4	25
38	Design, synthesis and biological evaluation of 4-anilinothieno[2,3-d]pyrimidine-based hydroxamic acid derivatives as novel histone deacetylase inhibitors. Bioorganic and Medicinal Chemistry, 2014, 22, 6146-6155.	3.0	24
39	Forrestiacidsâ€A andâ€B, Pentaterpene Inhibitors of ACL and Lipogenesis: Extending the Limits of Computational NMR Methods in the Structure Assignment of Complex Natural Products. Angewandte Chemie - International Edition, 2021, 60, 22270-22275.	13.8	24
40	AMPK-mediated phosphorylation on 53BP1 promotes c-NHEJ. Cell Reports, 2021, 34, 108713.	6.4	23
41	Targeted fluorescence imaging enhanced by 2D materials: a comparison between 2D MoS ₂ and graphene oxide. Chemical Communications, 2016, 52, 9418-9421.	4.1	21
42	Supramolecular core–glycoshell polythiophene nanodots for targeted imaging and photodynamic therapy. Chemical Communications, 2017, 53, 9793-9796.	4.1	21
43	LGH00031, a novel ortho-quinonoid inhibitor of cell division cycle 25B, inhibits human cancer cells via ROS generation. Acta Pharmacologica Sinica, 2009, 30, 1359-1368.	6.1	20
44	Design, synthesis and biological evaluation of thienopyrimidine hydroxamic acid based derivatives as structurally novel histone deacetylase (HDAC) inhibitors. European Journal of Medicinal Chemistry, 2017, 128, 293-299.	5.5	19
45	D-A-D fluorogenic probe for the rapid imaging of amyloid β plaques inÂvivo. Dyes and Pigments, 2017, 136, 224-228.	3.7	19
46	A â€~Clicked' Tetrameric Hydroxamic Acid Glycopeptidomimetic Antagonizes Sugar-Lectin Interactions On The Cellular Level. Scientific Reports, 2015, 4, 5513.	3.3	18
47	Design, synthesis and biological evaluation of isoquinoline-based derivatives as novel histone deacetylase inhibitors. Bioorganic and Medicinal Chemistry, 2015, 23, 5881-5890.	3.0	17
48	Plasma levels of growth differentiation factor-15 are associated with myocardial injury in patients undergoing off-pump coronary artery bypass grafting. Scientific Reports, 2016, 6, 28221.	3.3	17
49	Interlocked supramolecular glycoconjugated polymers for receptor-targeting theranostics. Chemical Communications, 2016, 52, 3821-3824.	4.1	17
50	Forrestiacids C and D, unprecedented triterpene-diterpene adducts from Pseudotsuga forrestii. Chinese Chemical Letters, 2022, 33, 4264-4268.	9.0	17
51	Functional Role of Histidine in the Conserved His-x-Asp Motif in the Catalytic Core of Protein Kinases. Scientific Reports, 2015, 5, 10115.	3.3	16
52	N-Oxyamide-linked glycoglycerolipid coated AuNPs for receptor-targeting imaging and drug delivery. Chemical Communications, 2016, 52, 2284-2287.	4.1	16
53	Self-Assembled 2D Glycoclusters for the Targeted Delivery of Theranostic Agents to Triple-Negative Breast Cancer Cells. ACS Applied Materials & Interfaces, 2019, 11, 22181-22187.	8.0	15
54	Long-Wavelength AIE-Based Fluorescent Probes for Mitochondria-Targeted Imaging and Photodynamic Therapy of Hepatoma Cells. ACS Applied Bio Materials, 2021, 4, 7016-7024.	4.6	15

#	Article	IF	CITATIONS
55	Revisit of a dipropargyl rhodamine probe reveals its alternative ion sensitivity in both a solution and live cells. Analyst, The, 2013, 138, 7087.	3.5	14
56	Involvement of transcription factor XBP1s in the resistance of HDAC6 inhibitor Tubastatin A to superoxidation via acetylation-mediated proteasomal degradation. Biochemical and Biophysical Research Communications, 2014, 450, 433-439.	2.1	14
57	AMPK regulates anaphase central spindle length by phosphorylation of KIF4A. Journal of Molecular Cell Biology, 2018, 10, 2-17.	3.3	14
58	A supramolecular pyrenyl glycoside-coated 2D MoS ₂ composite electrode for selective cell capture. Chemical Communications, 2016, 52, 11689-11692.	4.1	13
59	Supramolecular assembly of fluorogenic glyco-dots from perylenediimide-based glycoclusters for targeted imaging of cancer cells. Chemical Communications, 2017, 53, 11937-11940.	4.1	13
60	Supramolecular Polymer Dot Ensemble for Ratiometric Detection of Lectins and Targeted Delivery of Imaging Agents. ACS Applied Materials & Interfaces, 2017, 9, 3272-3276.	8.0	12
61	Photoswitchable arene ruthenium and pentamethylcyclopentadienyl rhodium complexes containing o-sulfonamide azobenzene ligands: Synthesis, characterization and cytotoxicity. Journal of Organometallic Chemistry, 2016, 820, 111-119.	1.8	11
62	Supramolecular glyco-poly-cyclodextrin functionalized thin-layer manganese dioxide for targeted stimulus-responsive bioimaging. Chemical Communications, 2018, 54, 4037-4040.	4.1	11
63	Protein Kinase A Rescues Microtubule Affinity-regulating Kinase 2-induced Microtubule Instability and Neurite Disruption by Phosphorylating Serine 409. Journal of Biological Chemistry, 2015, 290, 3149-3160.	3.4	9
64	Design and synthesis of benzylpiperidine inhibitors targeting the menin–MLL1 interface. Bioorganic and Medicinal Chemistry Letters, 2016, 26, 4472-4476.	2.2	9
65	GPCR Activation and Endocytosis Induced by a 2D Material Agonist. ACS Applied Materials & Interfaces, 2017, 9, 14709-14715.	8.0	9
66	Structurally diverse mono-/dimeric triterpenoids from the vulnerable conifer Pseudotsuga gaussenii and their PTP1B inhibitory effects. The role of protecting species diversity in support of chemical diversity. Bioorganic Chemistry, 2022, 124, 105825.	4.1	9
67	Discovery and characterization of a novel inhibitor of CDC25B, LGH000451. Acta Pharmacologica Sinica, 2008, 29, 1268-1274.	6.1	8
68	Mixed galactolipid anomers accentuate apoptosis of multiple myeloma cells by inducing DNA damage. Carbohydrate Research, 2015, 408, 114-118.	2.3	8
69	Supramolecular Assembly of TPEâ€Based Glycoclusters with Dicyanomethyleneâ€4 <i>H</i> â€pyran (DM) Fluorescent Probes Improve Their Properties for Peroxynitrite Sensing and Cell Imaging. Chemistry - A European Journal, 2020, 26, 14445-14452.	3.3	8
70	Stewartiacids A–N, C-23 carboxylated triterpenoids from Chinese Stewartia and their inhibitory effects against ATP-citrate lyase and NF-κB. RSC Advances, 2020, 10, 3343-3356.	3.6	8
71	Inner nuclear membrane protein TMEM201 promotes breast cancer metastasis by positive regulating TGFβ signaling. Oncogene, 2022, 41, 647-656.	5.9	8
72	Beshanzoides A–D, unprecedented cycloheptanone-containing polyketides from <i>Penicillium commune</i> P-4-1, an endophytic fungus of the endangered conifer <i>Abies beshanzuensis</i> . RSC Advances, 2021, 11, 39781-39789.	3.6	8

#	Article	IF	CITATIONS
73	Structural insights into the homology and differences between mouse protein tyrosine phosphatase-sigma and human protein tyrosine phosphatase-sigma. Acta Biochimica Et Biophysica Sinica, 2011, 43, 977-988.	2.0	7
74	Graphene oxide-enhanced cytoskeleton imaging and mitosis tracking. Chemical Communications, 2017, 53, 3373-3376.	4.1	7
75	Fluorescence imaging of a potential diagnostic biomarker for breast cancer cells using a peptide-functionalized fluorogenic 2D material. Chemical Communications, 2019, 55, 13235-13238.	4.1	7
76	Highly Oxygenated Triterpenoids and Diterpenoids from Fructus Rubi (Rubus chingii Hu) and Their NF-kappa B Inhibitory Effects. Molecules, 2021, 26, 1911.	3.8	7
77	5′-AMP-activated protein kinase (AMPK) regulates progesterone receptor transcriptional activity in breast cancer cells. Biochemical and Biophysical Research Communications, 2011, 416, 172-177.	2.1	6
78	The design of a novel near-infrared fluorescent HDAC inhibitor and image of tumor cells. Bioorganic and Medicinal Chemistry, 2020, 28, 115639.	3.0	6
79	Phosphoproteomics Reveals the AMPK Substrate Network in Response to DNA Damage and Histone Acetylation. Genomics, Proteomics and Bioinformatics, 2022, 20, 597-613.	6.9	6
80	Targeted delivery of maytansine to liver cancer cells <i>via</i> galactose-modified supramolecular two-dimensional glycomaterial. Chemical Communications, 2022, 58, 5029-5032.	4.1	6
81	Structurally diverse glycosides of secoiridoid, bisiridoid, and triterpene-bisiridoid conjugates from the flower buds of two Caprifoliaceae plants and their ATP-citrate lyase inhibitory activities. Bioorganic Chemistry, 2022, 120, 105630.	4.1	4
82	Identification of a new bis-amino acid glycoside selectively toxic to multiple myeloma cells. Carbohydrate Research, 2014, 394, 39-42.	2.3	3
83	Development of a novel H2S and GSH detection cocktail for fluorescence imaging. RSC Advances, 2016, 6, 59882-59888.	3.6	3
84	Targeted photoswitchable imaging of intracellular glutathione by a photochromic glycosheet sensor. Beilstein Journal of Organic Chemistry, 2019, 15, 2380-2389.	2.2	3
85	Identification of Bisindolylmaleimide IX as a potential agent to treat drug-resistant BCR-ABL positive leukemia. Oncotarget, 2016, 7, 69945-69960.	1.8	3
86	Phytochemical and biological studies on rare and endangered plants endemic to China. Part XXII. Structurally diverse diterpenoids from the leaves and twigs of the endangered conifer Torreya jackii and their bioactivities. Phytochemistry, 2022, 198, 113161.	2.9	3
87	Self-Assembled Thin-Layer Glycomaterials With a Proper Shell Thickness for Targeted and Activatable Cell Imaging. Frontiers in Chemistry, 2019, 7, 294.	3.6	1
88	Selective and sensitive fluorescence imaging reveals microenvironment-dependent behavior of NO modulators in the endothelial system. Journal of Pharmaceutical Analysis, 2020, 10, 466-472.	5.3	1
89	Synthesis and Biochemical Evaluation of 8H-Indeno[1,2-d]thiazole Derivatives as Novel SARS-CoV-2 3CL Protease Inhibitors. Molecules, 2022, 27, 3359.	3.8	1
90	Forrestiacidsâ€A andâ€B, Pentaterpene Inhibitors of ACL and Lipogenesis: Extending the Limits of Computational NMR Methods in the Structure Assignment of Complex Natural Products. Angewandte Chemie, 2021, 133, 22444-22449.	2.0	0